Volume 21
Number 30
14 August 2025
Pages 6015–6166

Soft Matter

rsc.li/soft-matter-journal

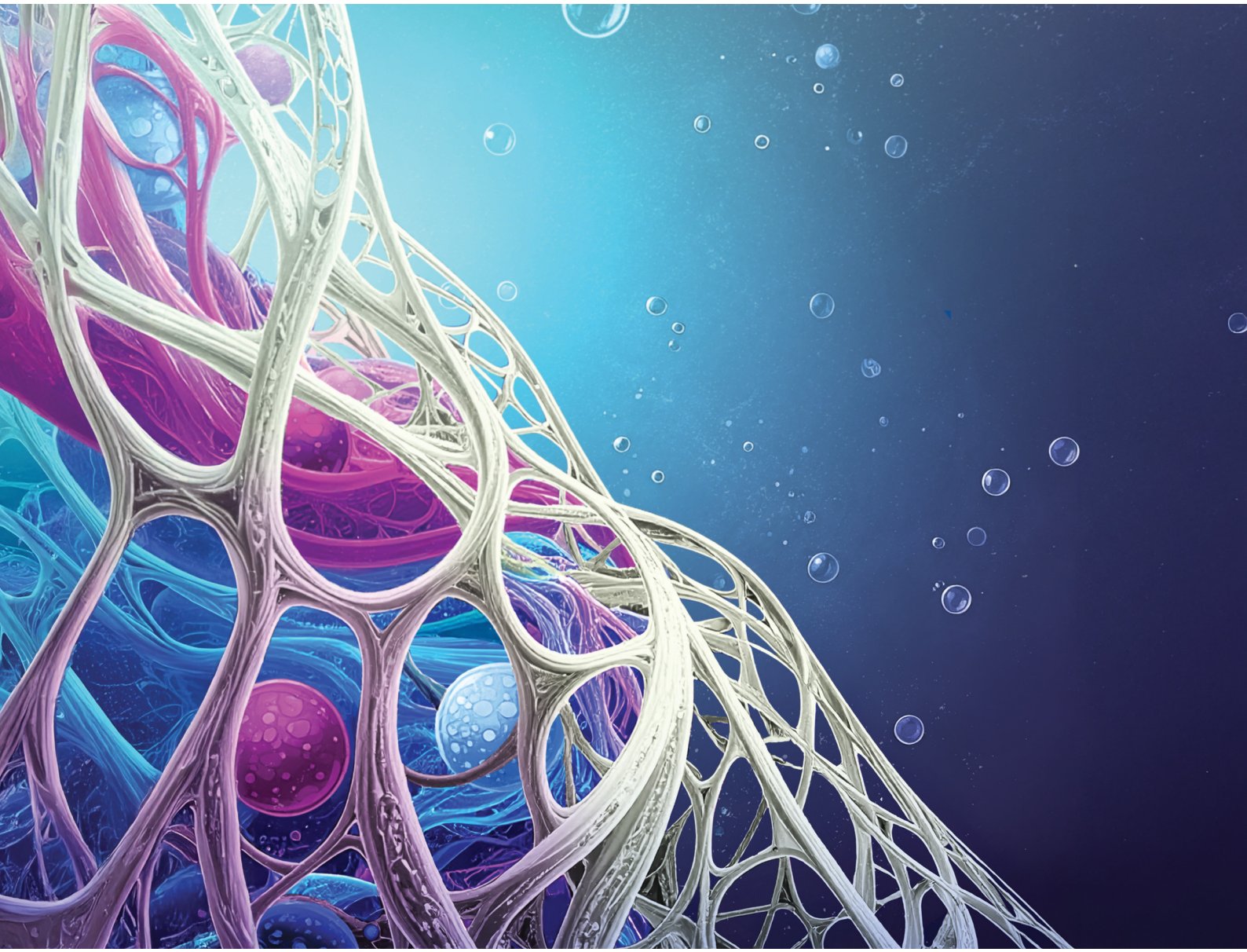

ISSN 1744-6848

ROYAL SOCIETY OF CHEMISTRY

PAPER
Emily R. Draper, Giacomo Picci *et al.*
Squaramide-based supramolecular gels for the removal of organic dyes from water matrices

20 YEARS ANNIVERSARY

Soft Matter

PAPER

View Article Online
View Journal | View Issue

Check for updates

Cite this: *Soft Matter*, 2025, **21**, 6047

Squaramide-based supramolecular gels for the removal of organic dyes from water matrices†

Jessica Milia,[a] Simona Bianco,[b] Tomás S. Plivelic,[c] Emily R. Draper,*[b] Giacomo Picci*[a] and Claudia Caltagirone[a]

Received 28th December 2024,
Accepted 27th February 2025

DOI: 10.1039/d4sm01538j

rsc.li/soft-matter-journal

A novel family of symmetric squaramide-based LMWGs has been synthesised, functionalized with both dansyl moieties and alkyl chain spacers of different lengths (n = 3 and n = 4 named **L1** and **L2**, respectively). **L1** and **L2** are able to form hydrogels in the DMSO : H_2O mixture in different ratios and concentrations. The gels obtained were characterized by means of rheology, TEM and small angle X-ray scattering (SAXS). Afterwards, the adsorption properties of these materials were studied and the gels were used for the removal of dyes, in particular Nile Blue A, Rose Bengal and Naphthol Yellow S from water samples. The reported results demonstrated the potential use of these materials for the removal of dyes in real polluted water matrices.

Open Access Article. Published on 07 March 2025. Downloaded on 5/27/2026 6:39:56 PM.
This article is licensed under a Creative Commons Attribution-NonCommercial 3.0 Unported Licence.

Introduction

During the last few decades, water pollution from several streams, including industrial waste, agricultural runoff, and mining activities, has become a devastating environmental issue.[1] Water pollution has a wide range of harmful effects on the environment, human health, and the economy.[2,3] In general, the consequences of water pollution are severe as 2 million tons of waste are released into water every day. 1.2 billion people suffer from the lack of drinking water, and the number of related deaths is more than 14 thousand people daily.[4] Among pollutants that contribute to water pollution, synthetic dyes are well-known contaminants and their effects on human health and the environment have been studied and documented over the past years.[5] Dyes are employed across various industrial sectors, including textiles, printing, plastics, food, cosmetics, and paper.[6] Their widespread use results in an annual dye production exceeding 700 000 tons. Despite stringent environmental regulations and advancements in dyeing techniques, over 15% of the total dye production is released into the environment each year.[7] Many dyes are heat resistant and do not decompose naturally. Moreover, some dyes and their byproducts are carcinogenic,[8] causing health disorders and destroying the aquatic life.[9] Several methods have been already used to remove dyes from water sources, which can be distinguished as physical methods, chemical methods and biological methods.[10,11] Among physical methods, the most used are adsorption, coagulation/flocculation and membrane filtration.[12,13] Concerning chemical methods, it is possible to use photocatalysis[14] or ozonation,[15] while the most common biological methods are enzymatic degradation[16] and biodegradation.[17] However, some of these methods are not commonly used due to their high costs.[18] Indeed, the scientific community is working towards the development of alternative solutions to treat wastewater by using low cost and non-toxic reusable materials.[19–22] In this context, supramolecular gels have been employed as adsorbent materials for water remediation.[23,24] Their large surface area and the presence of multiple functional groups in their porous structure make them versatile materials for these purposes.[25] Supramolecular gels are often based on low molecular weight gelators (LMWGs), which are small molecules able to self-assemble through non-covalent interactions, mainly hydrogen bond (H-bond) and π–π stacking interactions, trapping the solvent in a 3D structure.[26–28] Among H-bond donor scaffolds, ureas and amides have been extensively studied so far, while few examples of squaramide-based LMWGs have been reported in the literature.[29–38] In particular, squaramide-based supramolecular gels have been studied as multi-stimuli responsive materials[29,34] and as cell culture media.[31,33] Interestingly, to the best of our knowledge, no examples of supramolecular gels containing squaramide scaffolds as pollutant adsorbents from water matrices have ever been reported so far. Here, we report two LMWG symmetrical squaramides bearing a dansyl moiety and a C3 and a C4 alkyl chain spacer, namely **L1** and **L2** (Scheme 1). Gelation tests were carried out by testing different solvents and mixture of solvents, at different concentrations. The most stable gels obtained in the DMSO/water mixture were tested as adsorbent materials for the removal of three organic dyes Nile Blue A (NB), Rose Bengal (RB) and Naphthol Yellow S (NY) from

[a] *Dipartimento di Scienze Chimiche e Geologiche, Università degli Studi di Cagliari, S.S. 554 Bivio per Sestu, Monserrato 09042, CA, Italy. E-mail: gpicci@unica.it*
[b] *School of Chemistry, University of Glasgow, Glasgow, G12 8QQ, UK. E-mail: emily.draper@glasgow.ac.uk*
[c] *MAX IV Laboratory, Lund University, Lund, Sweden*

† Electronic supplementary information (ESI) available. See DOI: https://doi.org/10.1039/d4sm01538j

Open Access Article. Published on 07 March 2025. Downloaded on 5/27/2026 6:39:56 PM.
This article is licensed under a Creative Commons Attribution-NonCommercial 3.0 Unported Licence.

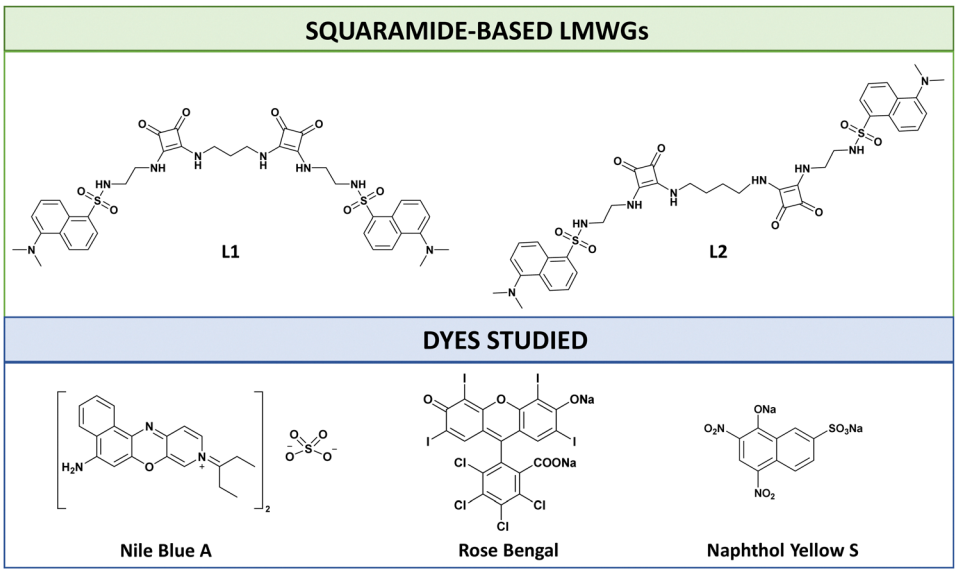

Scheme 1 LMWGs synthetized and dyes studied.

water (Scheme 1). NB is a synthetic azo dye used in textiles, known to cause skin irritation, lung cancer, allergic eye reactions, and inflammation.[39] NY is also known to be hazardous for the respiratory system, eyes and skin,[40] causing chemical conjunctivitis and blood cell abnormalities. Finally, RB is a mildly toxic dye adsorbed by compromised epithelial cells, mucus and fibrous tissues.[41–43] In this study, they have been chosen as "model compounds" with different electronic properties. Indeed, NY and RB are anionic, while NB is cationic. Moreover, due to the hydrophilic/hydrophobic properties of the three dyes (NB and RB are more hydrophobic than NY), their affinity towards the gel phase was also investigated. When water contaminated with the dyes is placed in contact with the gels the contaminants should be entrapped into the fibres of the material and removed from the matrices. To prove so, contact tests and flow tests were carried out to assess the adsorption abilities of the gels towards the selected dyes. The mechanical and morphological properties of the gels as well as their fibre structures and networks were investigated before and after the adsorption of dyes.

Results and discussion

Synthesis and characterization of gelators

Gelators **L1** and **L2** were synthesized following the synthetic procedures (Scheme S1) reported in the ESI.†[44] First, the dansyl derivative **1**, obtained by following a procedure reported in literature,[44] was reacted with 3,4-diethoxy-3-cyclobutene-1,2-dione in the presence of $Zn(Otf)_2$ as a catalyst in dry EtOH to obtain the monosubstituted squaramide **2**. Then, **2** was reacted with 1,3-diaminopropane or 1,4-diaminobutane to obtain **L1** and **L2**, respectively, in good yields (78–81%). **L1** and **L2** were fully characterised (see the ESI† for more details, Fig. S1–S3).

Gelation ability

The gelation ability of **L1–L2** was investigated by using two different triggers to promote the formation of gels, *i.e.* solvent and temperature triggers. Gelation tests were carried out at different concentrations in a wide range of solvents (tetrahydrofuran, acetonitrile, methanol, ethanol, 2-propanol, dimethyl sulfoxide (DMSO), and DMSO/water in various ratios, see ESI,† Table S1). Samples were sonicated, then heated with a heat gun to dissolve the solid and subsequently allowed to cool to room temperature (for temperature trigger). On the other hand, samples were sonicated and solubilized in a solvent in which they were completely soluble and then water was added as the antisolvent (for solvent trigger). All the gels studied in this work were obtained from a mixture of DMSO and water at different ratios and concentrations (see Table S1 in the ESI†).

Gel characterization

Gelators **L1–L2** were soluble in DMSO, whilst insoluble in all the other tested solvents. Interestingly, both the gelators formed gels in different ratios of DMSO : water and at gelator different concentrations, from 0.5% w/v (critical gelation concentration for **L1**) to 2% w/v. As it is well known, the inversion tube test of the sample shows up the qualitative formation of the material, highlighting that the material does not affect the gravity force turning down the vial. However, the oscillatory sweep stress and the frequency sweep rheology measurements allow identifying the material obtained as supramolecular gel. These two tests are used in the determination of the two moduli G' (storage modulus) and G'' (loss modulus) for the solid-like and liquid-like behaviour, respectively, and the stability of the material obtained. The results for the **L1** and **L2** gels are summarized in the ESI,† Table S2. Interestingly, the stiffest material for **L1** was obtained in a mixture of DMSO : H_2O 1 : 1 (v/v) at 1% w/v. As shown in the picture of the inversion tube test reported in Fig. 1, the temperature trigger gel appeared as a lightly opaque pale-yellow material, whereas the

 This journal is © The Royal Society of Chemistry 2025

Open Access Article. Published on 07 March 2025. Downloaded on 5/27/2026 6:39:56 PM.
This article is licensed under a Creative Commons Attribution-NonCommercial 3.0 Unported Licence.

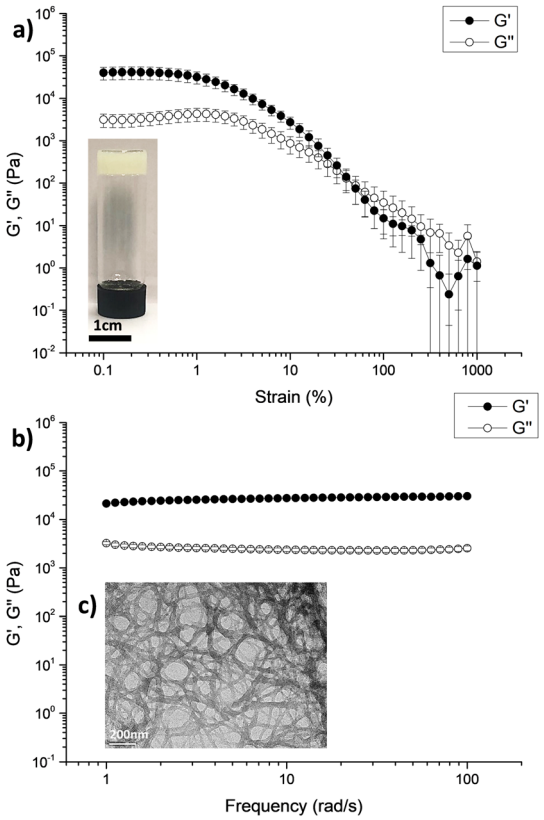

Fig. 1 Rheology and inner morphology characterization of the gel of **L1** in DMSO : H_2O (1 : 1 v/v) at 1% w/v, (a) strain sweep rheology analysis recorded at 10 rad s^{-1}, and the picture of the inversion tube test of gel (scale bar of 1 cm); (b) frequency sweep rheology analysis recorded at 10% strain; (c) TEM images (scale bar of 200 nm) that show entangled fibres in the gel. In all cases, error bars are obtained from triplicate measurements calculated through standard deviation.

oscillatory sweep stress rheology, along with the frequency sweep, highlighted the strong and stiff nature of the gel (G' = 41000 ± 5000 Pa and G'' = 3170 ± 970 Pa). Nevertheless, it is possible to note that the stiffness of the gel strongly depends on the amount of water in the solvent mixture. Indeed, the higher the amount of water in the solvent mixture, the softer the gel (see the ESI,† Table S2). These data indicate that even minor modifications in the preparation method can drastically change nanoscale characteristics and bulk-level properties.

To investigate the inner morphology of the gels, all the samples were dispersed in water, deposited in a carbon support film and dried for 24 hours in air to yield the xerogels which were then imaged by transmission electron microscopy (TEM). The images of the stiffest gel of **L1** (DMSO : H_2O 1 : 1 (v/v) 1% w/v) showed bundles of fibres, which may lead to a dense network and a strong material (Fig. 1c). The other gels of **L1** were also characterized by means of rheology and TEM analysis, and the results are reported in the ESI† (Fig. S4–S6 for rheology measurements and S11 for TEM images). It should be noted that drying can lead to artefacts and so characterisation of the structure and the network was also characterised by small angle X-ray scattering.[45]

As for **L1**, **L2** gels were obtained only in mixtures of DMSO and water at different concentrations (see the ESI,† Table S1). Particularly, **L2** was able to form a semi-transparent solvent trigger gel in DMSO : H_2O (1 : 1 v/v) at 0.5% w/v and two opaque temperature trigger gels, in a mixture of DMSO : H_2O (3 : 2 v/v) at 2% w/v and DMSO : H_2O (7 : 3 v/v) at 1.5% w/v. Unlike the gels obtained with **L1**, which are stable even for months, the gels obtained with **L2** are stable only for short periods of time not exceeding 48 hours (see the ESI,† Fig. S9 and S10). We hypothesised that this behaviour could be attributed to the presence of a C3 alkyl chain in the structure of **L1** that allows an ideal directionality of the H-bond donor and acceptor sites of two confined monomers, with the two dansyl moieties oriented towards the same direction. This structural feature probably promotes the formation of the 1D nanostructure representing the determining step for the formation of the entangled fibre structures. On the other hand, the presence of a C4 alkyl chain in the structure of **L2** might confer opposite features to the gelator, hampering the formation of a stiff and stable material.[46,47] Indeed, as shown in the time-dependent frequency sweep rheology reported in Fig. 2a the drop in rheological moduli observed after about 3 hours points out the lack in the stability of the material over time. On the other hand, the morphological analysis showed an entangled network of thick fibres for gels of **L2** (Fig. 2b), as well as different sizes and morphology of fibres, possible reason why samples were not stable for longer periods of time. The results of the

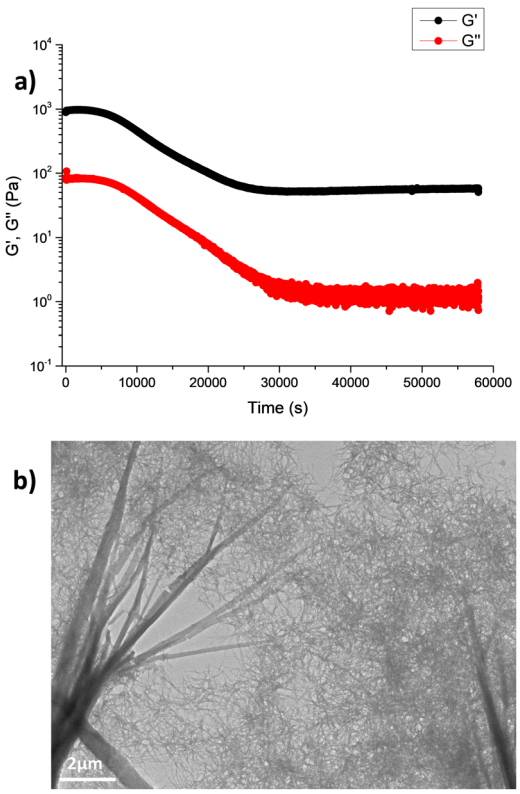

Fig. 2 (a) Time sweep of gel **L2**, DMSO : H_2O (1 : 1 v/v) at 0.5% w/v, (b) TEM images (scale bar of 2 µm) that show the presence of different size fibers.

Open Access Article. Published on 07 March 2025. Downloaded on 5/27/2026 6:39:56 PM.
This article is licensed under a Creative Commons Attribution-NonCommercial 3.0 Unported Licence.

morphological studies for the other gels with **L2** are reported in the ESI† (Fig. S12).

Overall, the values reported in Table S2 (ESI†) for the G' and G'' moduli for all the materials obtained highlight how **L1** formed the strongest gels (DMSO : H_2O (1 : 1 v/v) at 1% w/v) and was able to form hydrogel at low concentration (DMSO : H_2O (3 : 7 v/v) at 0.5% w/v), whereas **L2** expressed the tendency to form softer gels in solvent mixtures with higher water : DMSO ratios.

Small angle X-ray scattering (SAXS) was used to further characterize the gel fibre structure and network. This technique allowed us to understand the molecular packing of the aggregates in our supramolecular materials. Unlike TEM, used in this paper as a microscopic technique capable of providing us with information on the three-dimensional fibrous dried structure, SAXS can give us information on the structure of the 1-dimensional fibres making up the hydrated gel. By directly comparing the scattering data and fitting the data to models, we can understand how the molecules pack under different gelation conditions on the nanoscale.

Due to the lack of stability of **L2**, only **L1** was able to be analysed using SAXS (see Fig. 3 and the ESI,† Fig. S13 and Table S3). The SAXS data for all gels in different DMSO : H_2O ratios and different concentrations fit well to a flexible elliptical cylinder model, suggesting flexible tape-like fibres. In the case of **L1**, DMSO : H_2O (1 : 1 v/v) at 2% w/v and a polydispersity of 0.2 was added to better capture the data, which might be indicative of a slight heterogeneity in fibre radii making up the gel network. Across all samples, the radii were similar (40.7 Å in the case of gel **L1** DMSO : H_2O (3 : 7 v/v) 0.5% w/v, 42.1 Å for gel **L1** DMSO : H_2O (2 : 3 v/v) 1% w/v, 45.9 Å in the case of gel **L1** DMSO : H_2O (1 : 1 v/v) 1% w/v, and finally 45.1 Å in gel **L1** DMSO : H_2O (1 : 1 v/v) 2% w/v). As all the radii possess similar values, we hypothesise that the gelator forms similar structures in all gels, with subtle changes in molecular packing and interaction due to the different solvent ratios and concentrations. In all cases, the fitted models showed an axis ratio of around 2, indicative of the formation of wider elliptical fibres arising from the molecular structure of **L1** and similar molecular stacking in all four gels. Slight differences in length were further observed between the solvent-triggered gel **L1** in DMSO : H_2O (3 : 7 v/v) at 0.5% w/v and the other three temperature-triggered gels. These data suggest that longer structures are formed through the temperature trigger with lengths up to 200 nm, whereas the structures formed *via* solvent-switch show lengths of around 100 nm (Table S3, ESI†). Furthermore, the solvent-triggered gel showed a larger Kuhn length compared to the temperature-triggered ones, indicating the formation of more rigid structures possibly as a result of the different gelation triggers (Fig. 3).

Adsorption of dyes

To evaluate the potential application of **L1** and **L2** gels as adsorbent materials, the most stable gels were tested as potential candidates for the adsorption of dyes from water matrices, in particular NB, RB and NY. This set of dyes was chosen for their different properties, as already discussed in the Introduction. In this section, the term free gel will be used to indicate the samples formed without the presence of dyes. Two different experimental setups were developed by using the

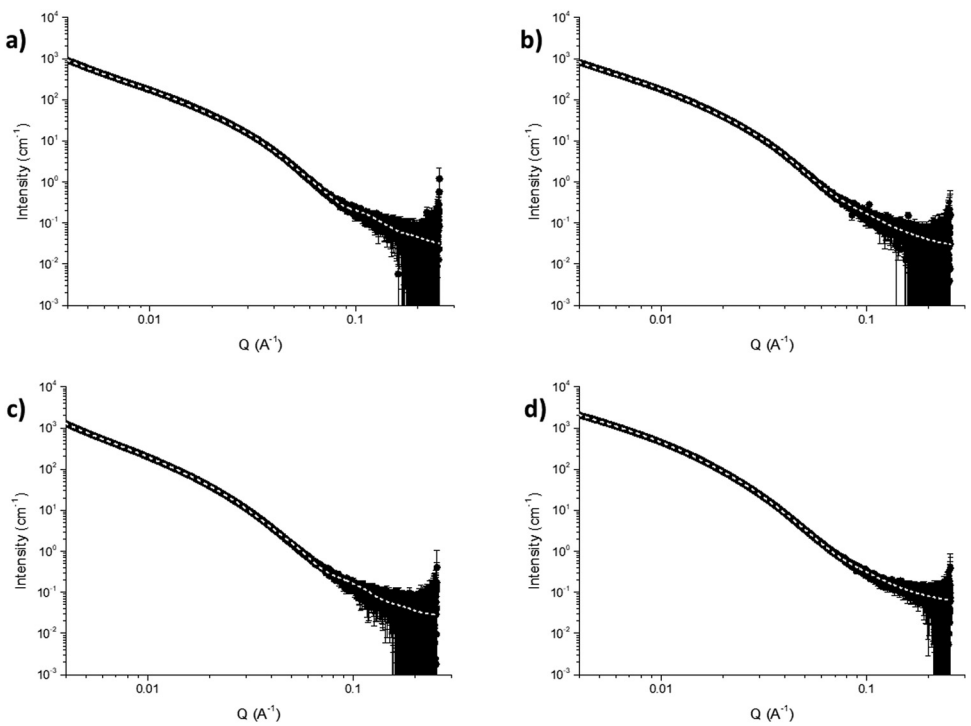

Fig. 3 (a) SAXS data for gel **L1** in DMSO : H_2O (3 : 7 v/v) at 0.5% w/v, (b) SAXS data for **L1** (DMSO : H_2O (2 : 3 v/v) at 1% w/v), (c) SAXS data for **L1** DMSO : H_2O (1 : 1 v/v) at 1% w/v and (d) SAXS data for **L1** DMSO : H_2O (1 : 1 v/v) at 2% w/v.

 This journal is © The Royal Society of Chemistry 2025

Open Access Article. Published on 07 March 2025. Downloaded on 5/27/2026 6:39:56 PM.
This article is licensed under a Creative Commons Attribution-NonCommercial 3.0 Unported Licence.

same condition and volume ratio between gels and dye solutions (1 : 2 v/v). In this endeavour, gels were prepared in vials (500 μL) by using both triggers, temperature and change of solvent, allowed to rest for a few hours before starting adsorption tests by putting them in contact with a dye water solution (1 mL). Among all the gels tested, **L2** gels in DMSO : H_2O (3 : 2 v/v) at 2% w/v and DMSO : H_2O (7 : 3 v/v) at 1.5% w/v were too weak and unstable to be brought in contact with aqueous solutions containing dyes and, thus, were not tested.

The amount of pollutant removed from the water solution was monitored by UV-vis measurements at different timepoints (1 h, 3 h, 5 h, 12 h, 24 h, and 48 h), comparing the data recorded with those carried out by the calibration curves of the studied dyes (see Fig. S14–S16 reported in the ESI†).

Indeed, by using the equation obtained from the calibration curve, the concentration of adsorbed dyes was calculated.

The removal efficiency (RE) of the dyes was calculated by using eqn (1) as follows:

$$\mathrm{RE}\ (\%) = \frac{(C_0 - C_f)}{C_0} \times 100 \qquad (1)$$

where C_0 is the initial concentration of the pollutant and C_f is the concentration of the pollutant in the eluted solution.

The RE(%) of gels after 48 hours of contact (time needed to observe the highest percentage of pollutant removal) are summarized in the ESI,† Table S4. The results highlighted how the best RE% was obtained with **L1** gel in DMSO : H_2O (3 : 7 v/v) at 0.5% w/v. Indeed, as shown in Fig. 4, this gel was able to remove up to 75.2% and 93.3% of NB and RB, respectively from the water dye solutions, whereas the RE% towards NY was found to be only about 40% of the dye adsorbed by the material. Moreover, for all the other tested gels, the same trend of RE% was found, even if with lower percentage of dye removal (see the ESI,† Fig. S17–S28 for the dye adsorption results for **L1** in (DMSO : H_2O (2 : 3 v/v), 1% w/v), (DMSO : H_2O (1 : 1 v/v), 1% w/v), and for **L2 in** DMSO : H_2O (1 : 1 v/v) at 0.5% w/v). The scarce adsorption of NY could be related to the high hydrophilicity of this molecule. The mechanical properties of the gels were investigated after dye adsorption, to evaluate if the dyes weaken or strengthen the materials. Strain sweep measurements were performed with the gels put in contact with the dye solutions for 48 hours. Interestingly, an increase in the linear viscoelastic region (LVR) was observed after the adsorption of all the three dyes used in the case of the **L1** gel in a mixture of DMSO : H_2O (3 : 7 v/v) at 0.5% w/v. Indeed, as shown in Fig. 4d, a doubling of strain percentage of the free

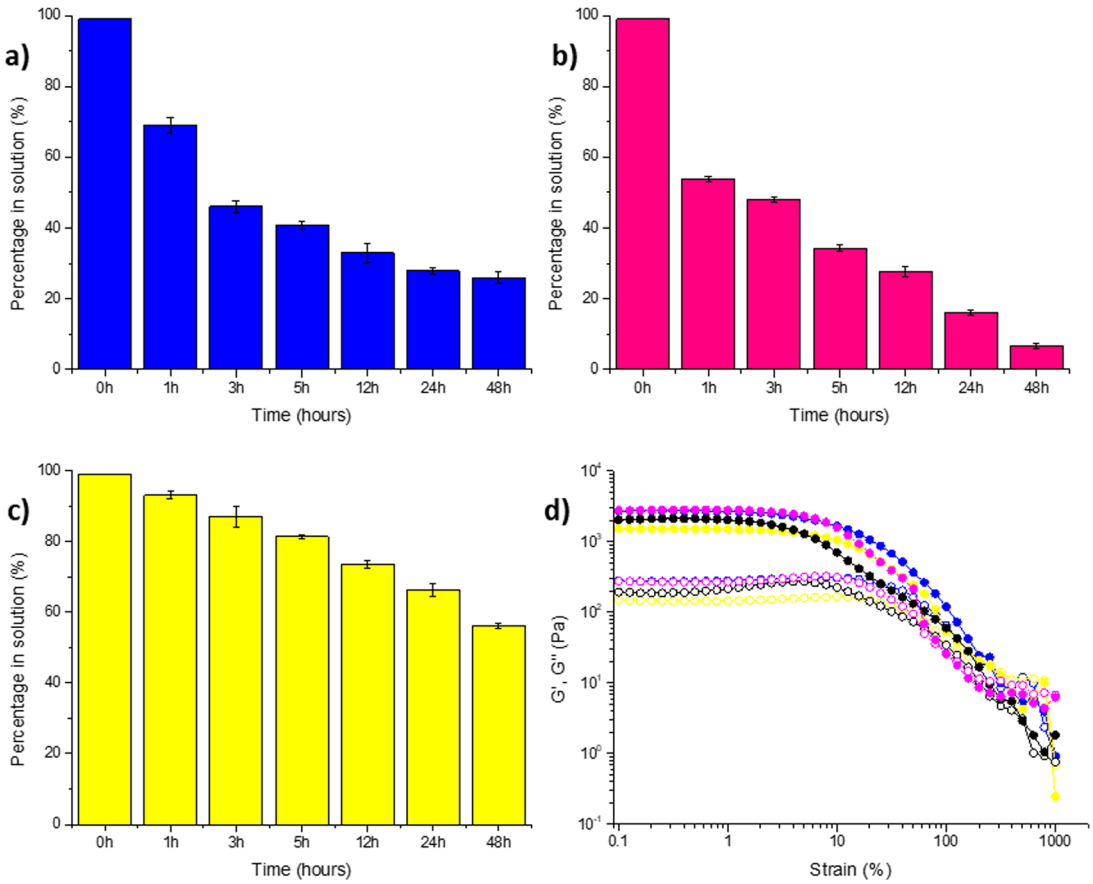

Fig. 4 Histograms of dye adsorption results for **L1** in DMSO : H_2O (3 : 7 v/v), 0.5% w/v in the presence of (a) NB, (b) RB, (c) NY and (d) strain sweep of **L1** in DMSO : H_2O (3 : 7 v/v) at 0.5% w/v after dye adsorption (full points indicate G' and empty points indicate G'', black points represent free gels, blue points represent gels in the presence of NB, yellow points represent gels in the presence of NY and pink points represent gels in the presence of RB).

Open Access Article. Published on 07 March 2025. Downloaded on 5/27/2026 6:39:56 PM.
This article is licensed under a Creative Commons Attribution-NonCommercial 3.0 Unported Licence.

gel (γ = 3.5%) was observed after the adsorption of the dye (γ = 7.5–8%). Furthermore, the adsorption of NB and RB caused an increase of G' values (from ~2000 Pa to ~3000 Pa), suggesting a stiffening of the gels after dye adsorption. The measurements performed for all the other tested gels are reported in the ESI,† Fig. S29, excluding the **L2** gel that converted to sol phase upon the contact with the dye water solutions.

The possible release of the gel components, gelator or DMSO, in water solution was evaluated by quantitative ^{1}H-NMR spectroscopy, by using maleic acid as an internal standard (2×10^{-2} M in D_2O).[48] The data reported in the ESI† (Fig. S30–S33) evidenced no gelator release, while a certain amount of DMSO (between 14.2% and 24.5%) switched into the water solution after 48 h.

Encouraged by these results, these gels were tested as potential filters for dye pollutants by using a second setup, called ''flow test''. Indeed, gels were first prepared in syringes (sealing the bottom with parafilm or cotton both removed before starting the analysis), allowed to rest for 2–3 hours to stabilize them, assessing the formation of the gel by inverting the syringe (see ESI,† Fig. S34a and S35a). Once formed, the gel was eluted with a water solution containing the target pollutant (gel : water solution 1 : 2 v/v), yielding a clearly discoloured solution exploiting only the atmospheric pressure as an experimental pump. The collected solution was then measured by UV-vis absorption spectroscopy and the RE% was calculated by using eqn (1) as already described above. Under these experimental conditions, all the gels studied were able to efficiently remove RB and NB after just one elution cycle, whereas in the case of NY, several cycles were needed to reduce the percentage of dye in solution, and the complete removal was not observed. For this reason, we deeply investigated the potential application of these materials, as well as their reuse for a repeated sequence of cycles, only towards NB and RB, to simulate the real application of these materials as filters for water treatment. The results of the RE% calculated over several elution cycles for all the gels tested are summarized in the ESI,† Tables S5 and S6. All gels were able to be reused for at least 3 cycles (in the case of both gels of **L1** and **L2** at 0.5% w/v), without intermediate washing, before losing their adsorption efficiency. Notably, the best performance was achieved for the gel of **L1** in DMSO : H_2O (1 : 1 v/v) at 1% w/v. Indeed, as reported in Table 1, upon elution with a water solution containing NB and RB (1.2×10^{-5} M and 1.1×10^{-5} M, respectively), the material was able to remove almost quantitatively the RB for 5 cycles and NB for 3 cycles. It is worth noting that the RE% was calculated to be around 70% also for further cycles. Furthermore, as shown in Fig. 5 for the test performed with **L1** in DMSO : H_2O (1 : 1 v/v) at 1% w/v in the presence of RB, the removal efficiency can be appreciated also by the naked eye, as the collected solution became colourless upon the elution, until the sixth elution cycle (Fig. 5c and b), and the dye layered on the surface of the material making it hot pink (Fig. 5d). The results obtained for **L1** in (DMSO : H_2O (3 : 7 v/v) at 0.5% w/v), **L1** in (DMSO : H_2O (2 : 3 v/v) at 1% w/v), and for **L2** in DMSO : H_2O (1 : 1 v/v) at 0.5% w/v are reported in Fig. S36–S39. The possible leach out of the gelator or loss of DMSO from the gels during the flow tests was evaluated by means of quantitative ^{1}H-NMR. As shown in the ESI,† Fig. S44, the elution of the gel with a solution of D_2O caused the release of 15.1% of DMSO from the gel of **L1** in DMSO : H_2O (1 : 1 v/v) at 1% w/v. Interestingly, upon a further elution of the same gel with D_2O, only 4.4% of DMSO was released (see the ESI,† Fig. S45). In both cases, as well as for the other tested gels, no significant release of the gelator was observed. Indeed, rheological strain tests performed on the washed gels evidenced that the mechanical properties of the material were not affected by the partial loss of DMSO, as well as the fibrous nature of the gel confirmed by the TEM images (see the ESI,† Fig. S48 and S49 for rheology and TEM, respectively, on the washed gels). With this in mind, to avoid the release of a significant amount of DMSO during the test, the flow tests were repeated on the materials washed with fresh water (in a double volume with respect to the volume of the gel).

Table 1 RE% results for **L1** gel in DMSO : H_2O (1 : 1 v/v) at 1% w/v after dye adsorption

	Rose Bengal (%)	Nile Blue A (%)
Cycle 1	98.7	97.5
Cycle 2	97.7	91.9
Cycle 3	97.6	89.3
Cycle 4	97.5	87.6
Cycle 5	96.7	84.3
Cycle 6	85.3	73.9
Cycle 7	73.9	—
Cycle 8	66.4	—
Cycle 9	52.4	—
Cycle 10	40.4	—

All washed gels tested were found to be more efficient towards the removal of RB than the unwashed gels. Surprisingly, the results summarised in the ESI,† Tables S7 and S8 highlighted how the gel of **L1** in DMSO : H_2O (3 : 7 v/v) at 0.5% w/v (the least concentrated) was able to dramatically improve its RE% towards both the target pollutants. Indeed, a RE% of $\geq$90% was achieved for 7 and 6 consecutive elution cycles in the case of the water solution containing NB and RB, respectively, compared to 1 and 4 cycles achieved with the unwashed gel. On the other hand, no significant enhancement of the removal efficiency towards NB was found in the case of gels of **L1** in DMSO : H_2O (2 : 3 v/v) at 1% w/v and **L1** in DMSO : H_2O (1 : 1 v/v) at 1% w/v (see the ESI,† Fig. S50–S53 for the dye adsorption results for the other gels studied).

With all these results in mind, we tried to regenerate the raw materials with the aim to prove their recyclability.

We attempted to wash the gels with a fresh water solution or small amounts of organic solvents, such as acetone, ethanol, or methanol. However, the addition of fresh water caused a negligible release of the pollutant adsorbed by the material, while the organic solvents were only able to remove a small amount of the dyes, as the material remained coloured, suggesting that a larger quantity of organic solvents might be required. Moreover, after several cycles of solvent addition, we observed that the gel started to collapse due to its solubility in the solvent or mechanical stress.

 This journal is © The Royal Society of Chemistry 2025

Open Access Article. Published on 07 March 2025. Downloaded on 5/27/2026 6:39:56 PM.
This article is licensed under a Creative Commons Attribution-NonCommercial 3.0 Unported Licence.

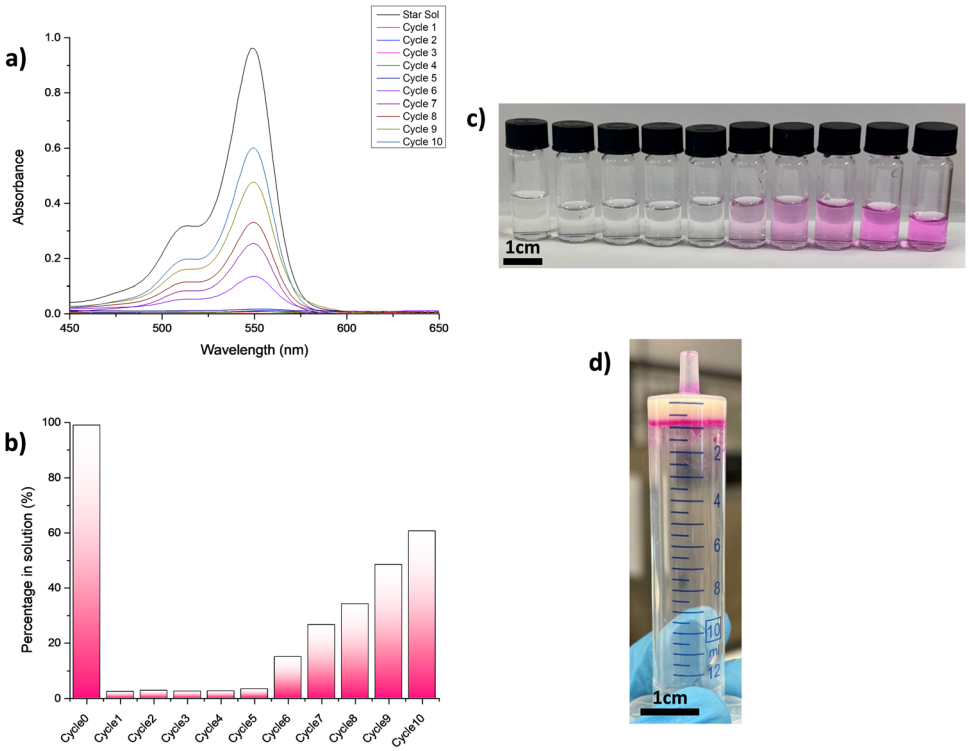

Fig. 5 (a) Absorbance spectra of filtered solution of RB (1.1×10^{-5} M starting solution), (b) histogram of dye amount in the filtered solution, (c) colour change of filtered solutions (scale bar of 1 cm) and (d) inversion tube test of **L1** gel in DMSO : H_2O (1 : 1 v/v) at 1% w/v after RB removal (scale bar of 1 cm).

SAXS measurements were useful to understand how the nanoscale structure of our soft materials changed following the adsorption of pollutants. These analyses were performed only in the presence of NB and RB, which were found to be the dyes adsorbed in the greatest quantities. Two experiments were recorded at different capillary depths. The first was recorded in the middle of the capillary where the gel completely adsorbed the dyes and the second was recorded at a height of 3 or 5 mm at the interface between the gel and the dye-containing solution (all fitting data are shown in the ESI,† Fig. S54 and S55 and Tables S9–S11). The SAXS data obtained in the middle of the gel showed no significant changes in the samples when compared with the free gel (Fig. 6, black, light pink and light blue), fitting to flexible elliptical cylinder models with similar values. The only exception was observed for gel **L1** in DMSO : H_2O (3 : 7 v/v) at 0.5% w/v, with the data fitting best elliptical cylinder models in the presence of dyes. The data suggested that for gels **L1** in DMSO : H_2O (2 : 3 v/v) 1% and **L1** in DMSO : H_2O (1 : 1 v/v) at 1% w/v, the dyes are likely stuck in the pores of the gel network and therefore do not affect the morphology of the primary fibres. This is further confirmed by rheology, as no differences in rheological behaviour were observed in the gels after dye adsorption (Fig. S29, ESI†). On the other hand, for gel **L1** in DMSO : H_2O (3 : 7 v/v) at 0.5% w/v, the change in fit can be related to a change in molecular packing, presumably due to interactions between the dye and the fibres. The gels were fitted to elliptical cylinder models with axis ratios between 2.5 and 3 (Tables S9–S11 and Fig. S54 and S55, ESI†), indicating that the primary fibres become considerably less flexible and more elliptical after interaction with both dyes. Similar changes in molecular packing in the presence of hydrophobic additives have previously been observed.[49,50] The change in structure also appeared to affect the rheological properties of the gels, which showed an increase in stiffness (G') and in the LVR (linear viscoelastic region) (Fig. 4d).

The SAXS data of samples, collected at the interface between the gel and the dye, appeared to change in the case of **L1** gels in DMSO : H_2O (3 : 7 v/v) at 0.5% w/v, **L1** gels in DMSO : H_2O (2 : 3) at 1% w/v and DMSO : H_2O (1 : 1) at 1% w/v in the presence of NB. In these samples, transitions from the flexible elliptical cylinder model to elliptical or simple cylinder models were observed. In the presence of RB at 3 mm height of the capillary, the only change observed was in the case of **L1** gels in DMSO : H_2O (3 : 7 v/v) at 0.5% w/v, which transitioned from a fitting of a flexible elliptical cylinder model to a fitting of an elliptical cylinder model. Transitions from flexible elliptical cylinders to cylinders or elliptical cylinders at this capillary depth could be due to the partial solubilization of the gels at the point where the solution comes in contact with the gel surface, resulting in higher interactions between the gel fibres and the dyes. This behaviour at the interface cannot be observed by rheology analysis since it provides information at the bulk level. Overall, we can infer that when the dye is interacting more with the fibre, slight changes in the SAXS and rheology can be observed, whereas it can be hypothesised that no changes occur when the dye is physically trapped or interacting very little with the gel fibres.

Open Access Article. Published on 07 March 2025. Downloaded on 5/27/2026 6:39:56 PM.
This article is licensed under a Creative Commons Attribution-NonCommercial 3.0 Unported Licence.

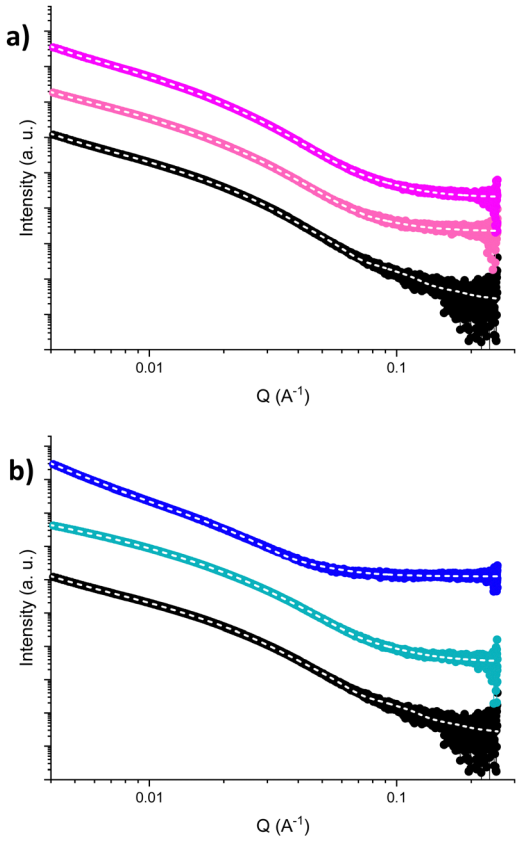

Fig. 6 SAXS data of **L1** gel in DMSO : H_2O (1 : 1 v/v), at 1% w/v after the adsorption of (a) RB and (b) NB at different depths. The black points indicate the free gel, while light pink and light blue points indicate the gel in the presence of the corresponding dyes, and pink and blue indicate the measurement at 3 mm and 5 mm of depth, respectively. The fit is indicated by a dashed line.

Conclusions

Two new squaramide-based LMWGs **L1** and **L2** that formed stable hydrogels in the DMSO : H_2O mixture in different ratios (3 : 7, 2 : 3 and 1 : 1 v/v for **L1** and 1 : 1, 3 : 2, 7 : 3 v/v for **L2**) in different concentrations (from 0.5% w/v to 2% w/v) were reported. Supramolecular gels were obtained by using two different triggers which are temperature variation and solvent switching. After characterization *via* rheology and transmission electron microscopy (TEM), these new materials were successfully used for the removal of dyes, in particular NB, RB and NY from water matrixes. Two different experiments were performed. Contact tests have been used as a general screening method, highlighting an average adsorption of about 75.8% in the presence of RB, 59.8% in the presence of NB and finally only 47.3% in the presence of NY. The most stable gels, obtained with gelator **L1** in DMSO : H_2O (3 : 7 v/v) at 0.5% w/v, in DMSO : H_2O (2 : 3 v/v) at 1% w/v and in DMSO : H_2O (1 : 1 v/v) at 1% w/v and gelator **L2** in in DMSO : H_2O (1 : 1 v/v) at 0.5% w/v, were studied as filters by using the flow tests. The possible reuse of gels was investigated, highlighting that all gels studied could be used at least 3 cycles with both dyes selected (NB and RB), showing a good adsorption ability. The possible release of gelators and DMSO was studied by quantitative ^{1}H-NMR. To avoid the presence of DMSO in the treated water, all gels were washed before using them as filters. After confirming the stability of materials, all flow tests were repeated. Washed gels showed a better RE%, increasing the number of reusing cycles. The best removal efficiency has been observed in the presence of RB. The reported results demonstrated the potential use of these materials for the removal of dyes in real polluted water matrices. This work represents the first example of squaramide-based supramolecular gels used as adsorbent materials for the removal of dyes from aqueous matrices. Although preserving the stability of the gels in real wastewater could be challenging, as well as the selectivity and sensitivity are crucial factors in real water matrices, which often contain diverse contaminants, these findings highlight the potential of such materials for water purification applications, paving the way for future developments in sustainable and efficient pollutant removal strategies.

Experimental

Materials and methods

All the reagents and solvents were obtained from chemical reagent suppliers and used directly without further purification. **L1** and **L2** were synthesized by attempting several synthetic routes, trying to achieve the greenest method to get the gelators. All the experimental details of synthesis are provided in the ESI.†

Gels preparation

Gels were obtained by using two different triggers. The first trigger is temperature variation and a typical procedure for gel formation in mixed solution is as follows: the gelator was weighted onto a screw-capped 2.0 mL glass bottle and the correct amounts of DMSO and H_2O were added by using a 1000 μL Eppendorf micropipette and then the mixture was heated until a transparent solution was obtained. After standing for 3–4 min at room temperature, the solution gave a semi-transparent pale-yellow gel. The gels obtained by using temperature as a trigger are stable at room temperature for few months (max 6), which is observed only in the case of **L1**. The second trigger is solvent switching and a typical procedure for gel formation in mixed solution is as follows: the gelator was weighed onto a 7 mL sterling vial and the correct amount of DMSO was added by using a 1000 μL Eppendorf micropipette. Once the gelator was completely dissolved, the second solvent, the water, was added and left to diffuse. After 20 minutes, a transparent pale-yellow gel was obtained. This type of gel is stable at room temperature for 2–3 months, which is observed only in the case of **L1**. All the gels obtained by using **L2** as LMWGs are not stable for more than 48 hours.

^{1}H and ^{13}C NMR

^{1}H and ^{13}C NMR spectra were recorded on a Bruker Avance 600 spectrometer in DMSO-d_6 at 298 K. The multiplicity of a signal is indicated as s (singlet), d (doublet), t (triplet), dd (doublet of doublets), dt (doublet of triplets), td (triplet of doublets), q (quartet) and m (multiplet). Quantitative ^{1}H-NMR

This journal is © The Royal Society of Chemistry 2025

Open Access Article. Published on 07 March 2025. Downloaded on 5/27/2026 6:39:56 PM. This article is licensed under a Creative Commons Attribution-NonCommercial 3.0 Unported Licence.

spectra were recorded in D_2O at 298 K, by using maleic acid as an internal standard.[48] For the contact test, a volume of 500 μL of D_2O was put into contact for 48 hours with a 250 μL of gel. For the flow test, D_2O (500 μL) was flowed through the gel (250 μL) prepared in a syringe of 1 mL. The D_2O solution collected was then analysed by means ^{1}H-NMR spectroscopy upon the addition of 100 μL of internal standard (maleic acid, 2×10^{-2} M). The DMSO release was calculated by using eqn (2) as follows:

$$n_{\mathrm{DMSO,extr}} = n_{\mathrm{maleic\,acid}} \frac{I_{\mathrm{DMSO}}}{I_{\mathrm{maleic\,acid}}} \frac{N_{\mathrm{maleic\,acid}}}{N_{\mathrm{DMSO}}} \quad (2)$$

UV-vis

UV-vis spectra were recorded in quartz cuvettes (optical path length 1 cm). Absorption data were obtained with an Agilent Cary 60 UV-vis spectrophotometer. Data analyses were performed by using Origin.

Rheology

All rheological experiments were carried out on an Anton Paar Physica MCR 301 rheometer at a constant temperature of 298 K. For measurements two different geometries were employed: cup and vane geometry (ST10-4V-8.8/97.5-SN42404) at a gap height of 1.5 mm and parallel plat (PP12.5-PP25 mm) at a measuring distance of 1.0 mm. Strain sweeps were performed over the range of 0.01% to 1000% strain at a frequency of 10 rad s^{-1}. Frequency sweeps were taken at 0.1–0.5% strain while ramping up the frequency from 1 rad s^{-1} to 100 rad s^{-1}. Time sweeps were performed at 0.1% strain and 10 rad s^{-1} frequency. The samples were prepared the day before analysis, and all samples were prepared as previously described in a 2 mL volume in 7 mL Sterilin vials (solvent trigger gels) and in a 2 mL volume in 7 mL glass vials (temperature trigger gels). Strain sweep and frequency sweep were performed in triplicate.

Transmission electron microscopy

Gels were dispersed in water before cast onto glow discharged carbon coated grids. The solvent was evaporated under the ambient conditions for minimum 24 hours. TEM images were recorded on a TEM Jeol JEM 1400 Plus instrument at an accelerating voltage of 80 kV. The images were analysed by using the ImageJ program.

Small angle X-ray scattering

SAXS data were collected at the CoSAXS beamline at the diffraction limited 3 GeV storage ring at the MAX IV Laboratory in Sweden, under proposal number 20231638 An X-ray beam of 15 keV was used, with the camera length set at 4.5 m to achieve a q-range of 0.0027–0.26 $Å^{-1}$ (where $q = 4\pi/\lambda \sin(\theta)$, $\lambda = 0.8267$ Å and 2θ the scattering angle). The data were collected using an EIGER2 4M hybrid photon-counting pixel detector (Dectris AG). The gel samples were prepared directly in 1.5 mm borosilicate glass capillaries by transferring the DMSO/H_2O mixture immediately after mixing or heating. The samples were then left undisturbed for 24 hours prior to any measurements. For the dye absorption studies, solutions of the dyes were left in contact with the gel in the capillary for 24 hours before measuring. Two areas of the capillaries were measured to investigate the effect of the dye on the bulk gel and at the interface with the solution.

Pollutant removal experiments

Gels were tested for the adsorption of dye pollutants (Nile Blue A, Rose Bengal and Naphthol Yellow S). Two different experiment setups were investigated: (1) the gel was formed in a vial and the pollutant solution was casted on top of it. Different contact times were studied (1 h, 3 h, 5 h, 12 h, 24 h, and 48 h); (2) the gel was placed inside a syringe/column, and the pollutant solution was allowed to flow through the gel. The flow test has been continuously repeated for several cycles (from 8 to 10) on the same gel sample, without washing it between each cycle, by adding a new starting solution containing the same concentration of dye. The same experiment setup has been used after washing the materials with fresh water (in double volume with respect to the volume of the gel). The gel (1 mL) was placed inside a syringe/column and eluted with a solution of fresh water (2 mL). The stability of the material was measured by rheology and TEM analysis, and then the flow test on the washed gels was conducted as already described above. The final concentration of the dye in solution was calculated according to a linear fit determined with the calibration curves of each dye studied (see the ESI† for more details (Fig. S4–S6)).

Author contributions

Conceptualization: C. C., G. P., E. R. D. and J. M.; methodology: J. M., S. B., and T. S. P.; validation: J. M.; formal analysis: J. M. and S. B.; investigation: J. M., S. B.; resources: All; data curation: J. M. and S. B.; writing – original draft: J. M., S. B., G. P., C. C., and E. R. D.; writing – review & editing: All; visualization: J. M. and S. B.; supervision: E. R. D. and C. C.; funding acquisition: C. C. and E. R. D.

Data availability

The data supporting this article have been included as part of the ESI.†

Conflicts of interest

The authors confirm that there are no conflicts to declare.

Acknowledgements

J. M. are gratefully for the financial support from MIUR for her PhD scholarship (PON R&I 2014-2020 DOT1304455-2, CUP: F21B21005140007). S. B. thanks the University of Glasgow for funding. E. D. thanks the UKRI for funding (MR/V021087/01). All authors thank Andrea Ardu from CeSAR for TEM analysis. This study was carried out within the RETURN Extended Partnership and received funding from the European Union

Open Access Article. Published on 07 March 2025. Downloaded on 5/27/2026 6:39:56 PM. This article is licensed under a Creative Commons Attribution-NonCommercial 3.0 Unported Licence.

Next-GenerationEU (National Recovery and Resilience Plan – NRRP, Mission 4, Component 2, Investment 1.3 – D.D. 1243 2/8/2022, PE0000005). All authors acknowledge the MAX IV Laboratory for time on the CoSAXS beamline under proposal number 20231638. Research conducted at MAX IV, a Swedish national user facility, was supported by the Swedish Research council under contract 20188-07152, the Swedish Governmental Agency for Innovation Systems under contract 2018-04969 and Formas under contract 2019-02496. This work benefitted from the SasView software, originally developed by the DANSE project under NSF award DMR-0520547. We thank Fin Hallam Stewart for the help in collecting SAXS data.

References

1 R. P. Schwarzenbach, T. Egli, T. B. Hofstetter, U. Von Gunten and B. Wehrli, *Annu. Rev. Environ. Resour.*, 2010, **35**, 109–136.
2 L. Lin, H. Yang and X. Xu, *Front. Environ. Sci.*, 2022, **10**, 880246.
3 M. N. Faiz Norrrahim, N. A. Mohd Kasim, V. F. Knight, M. S. Mohamad Misenan, N. Janudin, N. A. Ahmad Shah, N. Kasim, W. Y. Wan Yusoff, S. A. Mohd Noor, S. H. Jamal, K. K. Ong and W. M. Zin Wan Yunus, *RSC Adv.*, 2021, **11**, 7347–7368.
4 S. Bolisetty, M. Peydayesh and R. Mezzenga, *Chem. Soc. Rev.*, 2019, **48**, 463–487.
5 R. Kant, *Nat. Sci.*, 2012, **04**, 22–26.
6 M. Rochkind, S. Pasternak and Y. Paz, *Molecules*, 2015, **20**, 88–110.
7 S. Dutta, S. Adhikary, S. Bhattacharya, D. Roy, S. Chatterjee, A. Chakraborty, D. Banerjee, A. Ganguly, S. Nanda and P. Rajak, *J. Environ. Manage.*, 2024, **353**, 120103.
8 J. A. Miller and E. C. Miller, *Adv. Cancer Res.*, 1953, **1**, 339–396.
9 B. Lellis, C. Z. Fávaro-Polonio, J. A. Pamphile and J. C. Polonio, *Biotechnol. Res. Innov.*, 2019, **3**, 275–290.
10 G. Bal and A. Thakur, *Mater. Today: Proc.*, 2021, **50**, 1575–1579.
11 T. Robinson, G. McMullan, R. Marchant and P. Nigam, *Bioresour. Technol.*, 2001, **77**, 247–255.
12 V. Golob, A. Vinder and M. Simonič, *Dyes Pigm.*, 2005, **67**, 93–97.
13 H. R. Rashidi, N. M. N. Sulaiman, N. A. Hashim, C. R. C. Hassan and M. R. Ramli, *Desalin. Water Treat.*, 2015, **55**, 86–95.
14 E. Nyankson, E. Nyankson, R. Amedalor, G. Chandrabose, M. Coto, S. Krishnamurthy and R. V. Kumar, *ACS Omega*, 2020, **5**, 13641–13655.
15 B. Mella, B. S. de, C. Barcellos, D. E. da Silva Costa and M. Gutterres, *Ozone: Sci. Eng.*, 2018, **40**, 133–140.
16 K. D. Mojsov, D. Andronikov, A. Janevski, A. Kuzelov and S. Gaber, *Adv. Technol.*, 2016, **5**, 81–86.
17 J. D. Sosa-Martínez, N. Balagurusamy, J. Montañez, R. A. Peralta, R. de, F. P. M. Moreira, A. Bracht, R. M. Peralta and L. Morales-Oyervides, *J. Hazard. Mater.*, 2020, **400**, 123254.
18 A. P. Lim and A. Z. Aris, *Rev. Environ. Sci. Biotechnol.*, 2014, **13**, 163–181.
19 J. Takeshita, Y. Hasegawa, K. Yanai, A. Yamamoto, A. Ishii, M. Hasegawa and M. Yamanaka, *Chem. – Asian J.*, 2017, **12**, 2029–2032.
20 G. Sriram, S. Thangarasu, K. Selvakumar, M. Kurkuri, N. R. Dhineshbabu and T. H. Oh, *Colloids Surf., A*, 2024, **685**, 133199.
21 W. Logroño, M. Pérez, G. Urquizo, A. Kadier, M. Echeverría, C. Recalde and G. Rákhely, *Chemosphere*, 2017, **176**, 378–388.
22 I. Kiran, T. Akar, A. S. Ozcan, A. Ozcan and S. Tunali, *Biochem. Eng. J.*, 2006, **31**, 197–203.
23 C. Rizzo, S. Marullo, P. R. Campodonico, I. Pibiri, N. T. Dintcheva, R. Noto, D. Millan and F. D'Anna, *ACS Sustainable Chem. Eng.*, 2018, **6**, 12453–12462.
24 C. Rizzo, J. L. Andrews, J. W. Steed and F. D'Anna, *J. Colloid Interface Sci.*, 2019, **548**, 184–196.
25 B. O. Okesola and D. K. Smith, *Chem. Soc. Rev.*, 2016, **45**, 4226–4251.
26 M. Liu, G. Ouyang, D. Niu and Y. Sang, *Org. Chem. Front.*, 2018, **5**, 2885–2900.
27 N. M. Sangeetha and U. Maitra, *Chem. Soc. Rev.*, 2005, **34**, 821–836.
28 E. R. Draper and D. J. Adams, *Chem*, 2017, **3**, 390–410.
29 J. Ramos, S. Arufe, H. Martin, D. Rooney, R. B. P. Elmes, A. Erxleben, R. Moreira and T. Velasco-Torrijos, *Soft Matter*, 2020, **16**, 7916–7926.
30 S. Mommer and S. J. Wezenberg, *ACS Appl. Mater. Interfaces*, 2022, **14**, 43711–43718.
31 C. Tong, T. Liu, V. Saez Talens, W. E. M. Noteborn, T. H. Sharp, M. M. R. M. Hendrix, I. K. Voets, C. L. Mummery, V. V. Orlova and R. E. Kieltyka, *Biomacromolecules*, 2018, **19**, 1091–1099.
32 S. D. Shinde, N. Kulkarni and B. Sahu, *ACS Appl. Bio Mater.*, 2023, **6**, 507–518.
33 C. Tong, J. A. J. Wondergem, M. Van Den Brink, M. C. Kwakernaak, Y. Chen, M. M. R. M. Hendrix, I. K. Voets, E. H. J. Danen, S. Le Dévédec, D. Heinrich and R. E. Kieltyka, *ACS Appl. Mater. Interfaces*, 2022, **14**, 17042–17054.
34 J. V. Alegre-Requena, M. Häring, I. G. Sonsona, A. Abramov, E. Marqués-López, R. P. Herrera and D. D. Díaz, *Beilstein J. Org. Chem.*, 2018, **14**, 2065–2073.
35 J. Schiller, J. V. Alegre-Requena, E. Marqués-López, R. P. Herrera, J. Casanovas, C. Alemán and D. Díaz Díaz, *Soft Matter*, 2016, **12**, 4361–4374.
36 T. Liu, L. van den Berk, J. A. J. Wondergem, C. Tong, M. C. Kwakernaak, B. ter Braak, D. Heinrich, B. van de Water and R. E. Kieltyka, *Adv. Healthcare Mater.*, 2021, **10**, 1–10.
37 C. López, M. Ximenis, F. Orvay, C. Rotger and A. Costa, *Chem. – Eur. J.*, 2017, **23**, 7590–7594.
38 S. Bujosa, E. Castellanos, A. Frontera, C. Rotger, A. Costa and B. Soberats, *Org. Biomol. Chem.*, 2020, **18**, 888–894.
39 N. Natasha, A. Khan, U. U. Rahman, N. Sadaf, M. Yaseen, R. A. Abumousa, R. Khattak, N. Rehman, M. Bououdina and M. Humayun, *ACS Omega*, 2024, **9**, 19461–19480.

 This journal is © The Royal Society of Chemistry 2025

Open Access Article. Published on 07 March 2025. Downloaded on 5/27/2026 6:39:56 PM.
This article is licensed under a Creative Commons Attribution-NonCommercial 3.0 Unported Licence.

40 R. Jain, V. K. Gupta and S. Sikarwar, *J. Hazard. Mater.*, 2010, **182**, 749–756.
41 M. Vinuth and H. S. B. Naik, *J. Environ. Anal. Toxicol.*, 2016, **06**, 1000355.
42 M. G. Hassan, M. A. Wassel, H. A. Gomaa and A. S. Elfeky, *Sci. Rep.*, 2023, **13**, 1–16.
43 H. Yang Fan, Z. Li Zhu, W. Long Zhang, Y. Jia Yin, Y. Ling Tang, X. Hua Liang and L. Zhang, *Eur. J. Med. Chem.*, 2020, **199**, 112394.
44 E. L. Doyle, C. A. Hunter, H. C. Phillips, S. J. Webb and N. H. Williams, *J. Am. Chem. Soc.*, 2003, **125**, 4593–4599.
45 L. L. E. Mears, E. R. Draper, A. M. Castilla, H. Su, Zhuola, B. Dietrich, M. C. Nolan, G. N. Smith, J. Doutch, S. Rogers, R. Akhtar, H. Cui and D. J. Adams, *Biomacromolecules*, 2017, **18**, 3531–3540.
46 S. Panja and D. J. Adams, *Chem. Soc. Rev.*, 2021, **50**, 5165–5200.
47 N. Fujita, Y. Sakamoto, M. Shirakawa, M. Ojima, A. Fujii, M. Ozaki and S. Shinkai, *J. Am. Chem. Soc.*, 2007, **129**, 4134–4135.
48 F. Malz and H. Jancke, *J. Pharm. Biomed. Anal.*, 2005, **38**, 813–823.
49 S. Bianco, L. Wimberger, Y. Ben-Tal, G. T. Williams, A. J. Smith, J. E. Beves and D. J. Adams, *Chem. – Eur. J.*, 2024, **30**, e202400544.
50 L. Thomson, R. Schweins, E. R. Draper and D. J. Adams, *Macromol. Rapid Commun.*, 2020, **41**, 2000093.